Causal analysis of cortical networks involved in reaching to spatial targets

John R. Iversen, Alejandro Ojeda, Tim Mullen, Markus Plank, Joseph Snider,
Gert Cauwenberghs, and Howard Poizner

***Abstract*— The planning of goal-directed movement towards targets in different parts of space is an important function of the brain. Such visuo-motor planning and execution is known to involve multiple brain regions, including visual, parietal, and frontal cortices. To understand how these brain regions work together to both plan and execute goal-directed movement, it is essential to describe the dynamic causal interactions among them. Here we model causal interactions of distributed cortical source activity derived from non-invasively recorded EEG, using a combination of ICA, minimum-norm distributed source localization (cLORETA), and dynamical modeling within the Source Information Flow Toolbox (SIFT). We differentiate network causal connectivity of reach planning and execution, by comparing the causal network in a speeded reaching task with that for a control task not requiring goal-directed movement. Analysis of a pilot dataset (n=5) shows the utility of this technique and reveals increased connectivity between visual, motor and frontal brain regions during reach planning, together with decreased cross-hemisphere visual coupling during planning and execution, possibly related to task demands.**

I. Introduction

Reaching movements to targets in space require the transformation of multiple spatial representations in order to plan successful target-directed actions. While brain regions that participate in planning and execution of reaches are generally known from extensive work in humans and non-human primates [1]–[5], the dynamics of the interaction among these regions is less well understood [6]. While electroencephalography (EEG) and magnetoencephalography (MEG) reveal a potentially rich source of information about dynamic interactions at the source level, much of this richness is lost using traditional sensor-based analysis of EEG, and the use of non-directional measures of functional connectivity.

This work was supported in part by NSF ENG-1137279 (EFRI M3C), NSF SMA-1041755, and ONR MURI Award No. N00014-10-1-0072.

JR Iversen is with the Institute of Neural Computation and Swartz Center for Computational Neuroscience, UC San Diego, La Jolla, CA 92093, USA jiversen@ucsd.edu

A Ojeda is with the Department of Electrical and Computer Engineering, UC San Diego, La Jolla, CA 92093, USA, and Syntrogi Inc. aojeda@eng.ucsd.edu

T Mullen is with the Department of Cognitive Science and Institute of Neural Computation, UC San Diego, La Jolla, CA 92093, USA tmullen@ucsd.edu

M Plank was with the Institute of Neural Computation, UC San Diego, La Jolla, CA 92093, USA and is now with Brain Products, Inc. Markus.Plank@brainproducts.com

J Snider is with the Institute of Neural Computation, UC San Diego, La Jolla, CA 92093, USA j1snider@ucsd.edu

G Cauwenberghs is with the Department of Bioengineering, Jacobs School of Engineering and Institute of Neural Computation, UC San Diego, La Jolla, CA 92093, USA gert@ucsd.edu

H Poizner is with the Institute of Neural Computation, UC San Diego, La Jolla, CA 92093, USA hpoizner@ucsd.edu

Here we apply several new analytic tools to better understand brain activity at the cortical source level, primarily focussing on analysis of directed causal information flow using SIFT (Source Information Flow Toolbox) [7], [8]. We seek to address the following question: What is the pattern of cortical network dynamics that is evoked during the planning and execution of a spatial reaching movement?

II. Methods

A. Participants, Task and EEG recording

Participants: Ten healthy, right-handed participants (age: 20.8 ± 2.6) participated in this study. Here we present the analysis of the first five participants. The study was approved by the Human Subjects Institutional Review Board of the University of California, San Diego. Written informed consent was obtained from all the subjects.

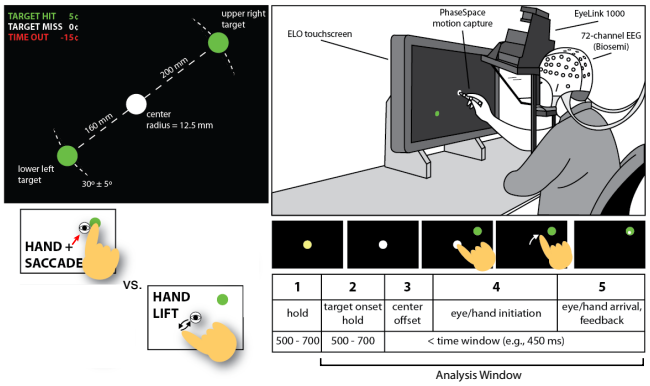

Fig. 1. Experimental setup and task design. Adapted from [9]

Task: Subjects sat in front of a touch screen and were asked to perform time-constrained reaching and eye movements from the center of the touch-screen to a lateral target as depicted in Fig. 1. Briefly, in reach trials a stylus was touched to a central fixation dock (Fig. 1). After 500-700 ms, a green target dot appeared in the upper right or lower left part of the screen. Participants held still until movement was triggered by the offset of the central fixation dock (500-700 ms after the target appeared). In Reach trials, participants made a rapid movement to reach and saccade to the target. In the control Lift condition, the stylus was lifted from the central dock, and the targets were irrelevant. We analyzed data from a time window that included a target identification and movement planning phase (0 to 500 ms after target appearance) as well as the actual movement (from

600-1000ms). The current analysis pools trials for both target directions, as we are interested in the general process of reach planning, rather than the specifics of target directions. Further details on the task are available in [9].

EEG recording: Scalp electroencephalographic activity was sampled continuously at 512 Hz using a 70-channel active electrode array, of which 64 channels were mounted in an elastic cap according to the extended Interna- tional 10-20 system, with a DRL/CMS reference (Biosemi Inc., Amsterdam, Netherlands). Electrode locations were digitized in 3-D space (Polhemus Inc., Colchester, VT, USA) for use in constructing head models (see below).

B. Analysis

Data analysis was conduced using the EEGLAB, BCILAB, and SIFT open source toolboxes for the analysis of EEG and MEG data [7], [8], [10], [11].

Independent Component Analysis: After bandpass filtering (1-55Hz) and average re-referencing, noisy trials and channels were manually excluded. The data were then decomposed using independent component analysis (ICA; infomax algorithm) to yield a set of maximally independent components, which are thought to represent spatially discrete processes within the brain, as well as biological artifacts (eye, muscle, heart), and noise components [12]. Those components that could be reliably modeled by a dipole source within the brain volume (average 14 brain components per individual) were included for further analysis [13], and a cleaned dataset consisting of activity only from these components was projected back to the channel level and down sampled to 128 Hz for use in subsequent processing.

Source Localization: Using the MoBILAB toolbox [14], an individualized head model was estimated for each participant by deforming the skin layer of a head model based on the MRI MNI Colin27 to match the digitized electrode locations, then warping the layers of the head model: brain, CSF, skull, and scalp to match subject's head shape [15]. The brain sourcespace for current source density localization was defined by a mesh of 4825 vertices corresponding to the cortex, and the lead field matrix was computed using the Boundary Element Method (BEM) using OpenMEEG [16]. For inverse modeling, which projects channel activity onto the cortical source space, we used anatomically constrained LORETA with Bayesian hyperparameter estimation [17]. This approach automatically controls the level of regularization in sensor and cortical space to minimize spurious sources and depth bias.

ROIs for causal analysis were selected with reference to an initial clustering (k=14) of independent components across participants to define regions of concentrated IC activity [8]. A set of 9 ROIs were chosen: bilateral inferior occipital (Occ), superior parietal (Par), and pre central gyrus motor (Mot) cortices and three midline ROIs: anterior cingulate cortex (ACC), supplementary motor area (SMA) and precuneus (Prec) which combined left and right hemispheres into a single ROI. The brain signal for each ROI was defined as the instantaneous median value of signals across each vertex of the ROI. Fig 2 shows the set of ROIs shown in this paper (following SIFT analysis, SMA and Prec showed no causal influence on the other ROIs structures using the SdDTF causal measure). Using common ROIs across participants considerably simplifies group comparisons of SIFT results, when compared to the traditional approach of examining connectivity among ICs, which can differ in number and location across subjects, and make network comparisons difficult [18].

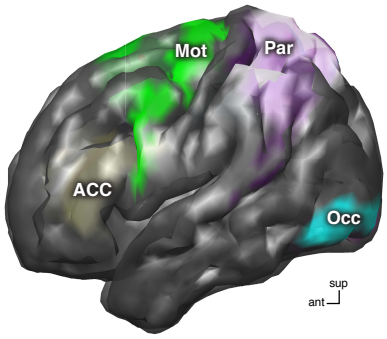

Fig. 2. Regions of interest used in the network analysis. ACC=Anterior Cingulate Cortex (on midline), Mot=Motor Cortex (pre central gyrus), Par=Parietal Cortex, Occ=Occipital Cortex.

SIFT: We applied routines from SIFT to model spatio-spectro-temporal multivariate causal interactions between epoched ROI time-series. Specifically, for each subject and condition, ROI data were pre-processed with local detrending to remove drift, followed by temporal and ensemble normalization. A linear vector (multivariate) autoregressive (VAR) model of order 15 was then fit to the multi-trial ensemble, in a 500 ms sliding window with a step size of 30 ms, using the Vieira-Morf lattice algorithm. Following model fitting and tests of stability and residual whiteness (autocorrelation function and Portmanteau), the Short-time Direct Directed Transfer Function (SdDTF) [19] was estimated from the VAR coefficients. The SdDTF captures time-varying connectivity by applying the dDTF to short, overlapping windows, and it it reflects only direct, not indirect, causal flows between two signals.

$$\eta_{ij}^2(f,t) = \frac{|H_{ij}(f,t)|^2 |P_{ij}(f,t)|^2}{\sum_{klf\tau} |H_{kl}(f,\tau)|^2 |P_{kl}(f,\tau)|^2}$$

where $H(f,t)$ is the MVAR transfer matrix and $P(f,t)$ is partial coherence, both for a window centered at t. Analogously to conditional spectral Granger causality, the SdDTF quantifies time-varying direct (conditional), directionally-specific information transfer between source processes at each frequency (here, 1-50 Hz).

III. Results

Mean causal information transfer (averaged across 5 participants and two conditions), as measured by the SdDTF is shown in Fig 3 as a matrix showing information transfer from each ROI (columns) to all other ROIs (rows). Each cell of the matrix shows the time-frequency distribution of information

transfer between a respective pair of ROIs, with highest information transfer indicated by warm colors. The most notable feature of the analysis is that occipital cortices (R and L Occ) are the strongest drivers of activity in other ROIs: They are most strongly coupled to each other (cells indicated by 'a' on the figure), but also demonstrate an influence on ACC (b), and left and right parietal cortices (c). The greatest information flow was seen in the lower frequencies (3-15Hz) which includes discrete theta and alpha bands. Weaker reciprocal connectivity is apparent from bilateral parietal to occipital cortices (d), and from left motor cortex (contralateral to the action hand) to ACC (e). The right parietal cortex was more strongly connected to the network than the left. SMA and precuneus (not shown) exerted no causal influence on these ROIs, although SMA was weakly causally influenced by left motor, bilateral occipital, and ACC, while the precuenus was weakly influenced by ACC.

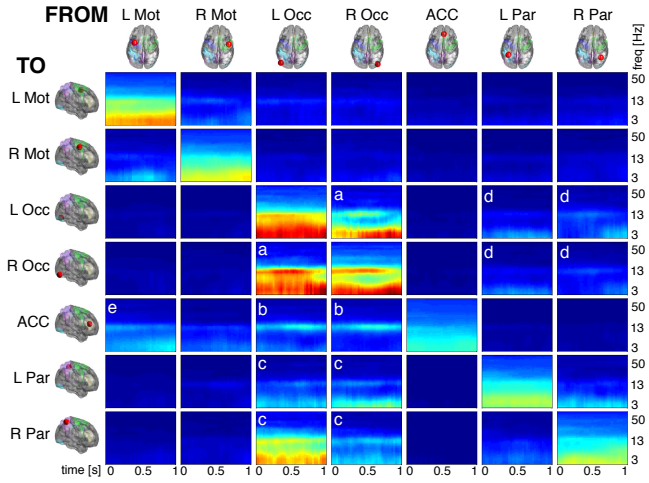

Fig. 3. Causal information flow analysis showing SdDTF magnitude from each ROI (columns) to other ROIs (rows) averaged across subjects and conditions. Each cell shows the SdDTF magnitude as a function of time and log-frequency. Information flow is greatest from Occipital (L Occ and R Occ) to other ROIs, particularly the contralateral Occpital cortex, the Anterior Cingulate Cortex (ACC) and bilateral Parietal Cortex (R Par > L Par). Panel labels are explained in the text.

The main question of interest in this study is how causal connections differ between the Reach condition, in which visually guided spatial reaching action is planned and executed, vs. the Lift condition in which there is no target-directed action. Fig. 4 shows the difference in information flow (Reach - Lift), with red indicating greater causal connectivity in the Reach condition, and blue indicating less causal connectivity in the reach condition. Differences are thresholded so that only the largest 2.5 % are shown. The largest differences are a decrease in reciprocal connectivity between occipital cortices during the Reach task (a), and an increase in connectivity from occipital cortices to the ACC (b), as well as from left motor cortex to the right motor cortex (c) and ACC (d). Differences in causal influence between occipital and parietal cortices were more variable. As with the mean connectivity, the differences lie primarily in the theta and alpha (5-15 Hz) frequency bands.

The temporal pattern of the differences provides additional insight when compared to the time course of each trial, which involved target identification and movement planning in the first 0.5 s, and movement execution in the second half of the trial. The occipital decoupling (a), occipital to ACC coupling (b), and motor driving in the theta band (c and d) were all larger during the planning period, while greater motor outflow (c and d) at higher frequencies in the low-beta band (15-25 Hz) was seen only during movement execution.

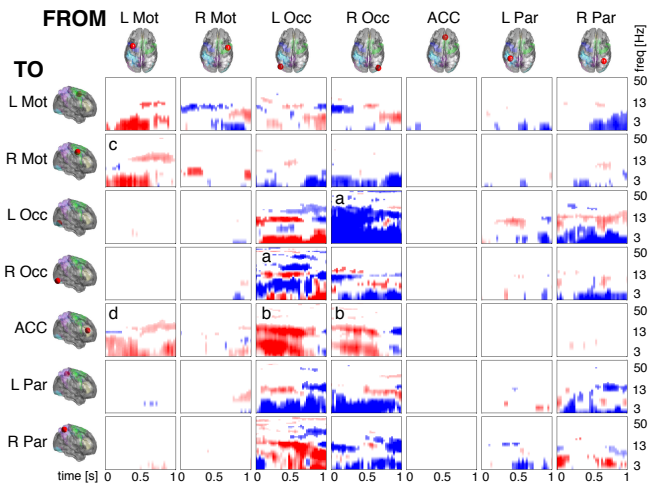

Fig. 4. Causal information flow *differences* between Reach and Lift conditions, Same conventions as Fig. 3. During reach planning (first half of trial, 0 to 0.5 s), there is greater information flow at lower (theta and alpha) frequencies between both occipital cortices and the ACC. Throughout reach trials, there is lower cross-hemisphere coupling between Occipital cortices in the alpha range. See text for further details.

IV. Conclusion

In this study, we examined cortical network directed information transfer during a visually-guided reaching task. Network connectivity findings are summarized in a 3D rendering of the network of ROIs in Fig. 5, with yellow and red colors showing links with greater connectivity in the directed Reach condition vs a non-directed control condition. In summary, there were two main findings of this pilot analysis: 1) The reach task increased causal flow into the anterior cingulate cortex from occipital and left motor cortices, and this increase was generally larger during the movement planning than the movement execution phase, and 2) there was greater cross-hemisphere decoupling of occipital cortices during the Reach task.

These results are largely in accord with existing knowledge, which implicates the parietal cortices in guiding action directed at visual targets [3], [20]. The observation that ACC was driven more strongly during reach planning is in accord with the proposal that the ACC is a primary locus for the translation of intention into action [21]. The occipital decoupling may be a more general phenomenon, related to task demands rather than reaching per-se. However, it is interesting to speculate on the utility of decoupling the two

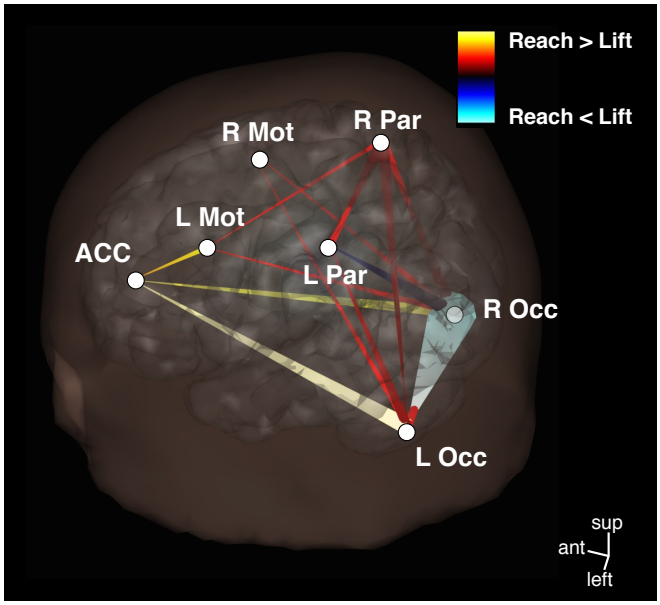

Fig. 5. Summary of connectivity differences between Reach and Lift conditions shown in a 3D (BrainMovie3D) rendering of a left-facing head. ROI centers are indicated by white dots and labels. Links between ROIs are colored to indicate if they have greater connectivity during Reach (yellows and reds) or less connectivity (blues). The diameter of the link indicates the magnitude of the difference and directionality is indicated by the direction of taper. Differences are averaged across 1-50 Hz, and at t = 375 ms. The network graph shows primarily the decoupling between Occipital cortices and greater connectivity between Occipital, ACC and left motor cortex in the Reach condition.

hemispheres when the task involves differentiating targets in opposite hemifields, and this could be investigated further by examining activation and causality differences as a function of target location.

This work provides demonstration of the utility of combining ICA, minimum-norm distributed source localization, and linear dynamical modeling to gaining insights about causal information flow within a network of cortical areas involved in visually-guided movements, and extends past work with this paradigm, which examined the encoding and modulation of EEG responses by different reaching modalities and target direction [9], [22], as well as the decoding of target direction from activity in parietal cortex [23]. In addition to enabling understanding of brain function, source information flow measures have potential application in brain computer interfaces, adding a new dimension of features relating to network connectivity, which could be useful, for example, in detecting network states corresponding to motion planning and the intent to move.

References

[1] Scott Glover, Matthew B Wall, and Andrew T Smith. Distinct cortical networks support the planning and online control of reaching-to-grasp in humans. *Eur J Neurosci*, 35(6):909–915, March 2012.

[2] Flavia Filimon. Human cortical control of hand movements: parietofrontal networks for reaching, grasping, and pointing. *neuroscientist*, 16(4):388–407, August 2010.

[3] Barbara Heider, Anushree Karnik, Nirmala Ramalingam, and Ralph M Siegel. Neural representation during visually guided reaching in macaque posterior parietal cortex. *J Neurophysiol*, 104(6):3494–3509, December 2010.

[4] P B Johnson, S Ferraina, L Bianchi, and R Caminiti. Cortical networks for visual reaching: physiological and anatomical organization of frontal and parietal lobe arm regions. *Cereb Cortex*, 6(2):102–119, March 1996.

[5] Y Burnod, P Baraduc, A Battaglia-Mayer, E Guigon, E Koechlin, S Ferraina, F Lacquaniti, and R Caminiti. Parieto-frontal coding of reaching: an integrated framework. *Experimental brain research*, 129(3):325–346, December 1999.

[6] Leighton B N Hinkley, Srikantan S Nagarajan, Sarang S Dalal, Adrian G Guggisberg, and Elizabeth A Disbrow. Cortical temporal dynamics of visually guided behavior. *Cereb Cortex*, 21(3):519–529, March 2011.

[7] Tim Mullen, Arnaud Delorme, Christian A Kothe, and Scott D Makeig. An Electrophysiological Information Flow Toolbox for EEGLAB. *Society for Neuroscience*, 2010.

[8] Arnaud Delorme, Tim Mullen, Christian A Kothe, Zeynep Akalin Acar, Nima Bigdely-Shamlo, Andrey Vankov, and Scott D Makeig. EEGLAB, SIFT, NFT, BCILAB, and ERICA: New Tools for Advanced EEG Processing. *Comput Intell Neurosci*, 2011:1–12, 2011.

[9] Cheolsoo Park, Markus Plank, Joe Snider, Sanggyun Kim, He Huang, Sergei Gepshtein, Todd Coleman, and Howard Poizner. EEG gamma band oscillations differentiate theplanning of spatially directed movements of thearm versus eye: multivariate empirical modedecomposition analysis. *IEEE Trans Neural Syst Rehabil Eng*, under revision:1–28, March 2014.

[10] Arnaud Delorme and Scott D Makeig. EEGLAB: an open source toolbox for analysis of single-trial EEG dynamics including independent component analysis. *J Neurosci Methods*, 134(1):9–21, March 2004.

[11] Christian A Kothe and Scott D Makeig. BCILAB: A BCI / EEG research framework. *Proceedings, Fourth International Brain-Computer Interface Meeting*, 2010.

[12] Scott D Makeig, Andrew J Bell, and Tzyy-Ping Jung. Independent component analysis of electroencephalographic data. *Adv Neural Info Proc Syst*, 8:145–151, 1996.

[13] Arnaud Delorme, Jason Palmer, Julie Onton, Robert Oostenveld, and Scott D Makeig. Independent EEG sources are dipolar. *PLoS ONE*, 7(2), 2012.

[14] Alejandro Ojeda, Nima Bigdely-Shamlo, and Scott D Makeig. MoBILAB: an open source toolbox for analysis and visualization of mobile brain/body imaging data. *Front Hum Neurosci*, 8, 2014.

[15] Pedro A Valds-Hernndez, Nicols von Ellenrieder, Alejandro Ojeda-Gonzalez, Silvia Kochen, Yasser Alemn-Gmez, Carlos Muravchik, and Pedro A Valds-Sosa. Approximate average head models for EEG source imaging. *J Neurosci Methods*, 185(1):125–132, December 2009.

[16] Alexandre Gramfort, Theodore Papadopoulo, Emmanuel Olivi, and Maureen Clerc. OpenMEEG: opensource software for quasistatic bioelectromagnetics. *Biomed Eng Online*, 9, 2010.

[17] Nelson J Trujillo-Barreto, Eduardo Aubert-Vzquez, and Pedro A Valds-Sosa. Bayesian model averaging in EEG/MEG imaging. *NeuroImage*, 21(4):1300–1319, April 2004.

[18] Wesley Thompson, Tim Mullen, Julie Onton, and Scott Makeig. A bayesian spatiotemporal model for multi-subject EEG source dynamics and effective connectivity. *Front Hum Neurosci Conference Abstract: XI International Conference on Cognitive Neuroscience (ICON XI)*, September 2011.

[19] Anna Korzeniewska, Ciprian M Crainiceanu, Rafa Ku, Piotr J Franaszczuk, and Nathan E Crone. Dynamics of event-related causality in brain electrical activity. *Hum Brain Mapp*, 29(10):1170–1192, October 2008.

[20] Sarah Shomstein and Steven Yantis. Parietal cortex mediates voluntary control of spatial and nonspatial auditory attention. *J Neurosci*, 26(2):435–439, January 2006.

[21] T Paus. Primate anterior cingulate cortex: where motor control, drive and cognition interface. *Nat Rev Neurosci*, 2(6):417–424, June 2001.

[22] Markus Plank, Steven A Hillyard, He C Huang, Joseph Snider, Sergei Gepshtein, and Howard Poizner. EEG correlates of spatially-directed movements of the hand and eyes during rapid reaching under risk and uncertainty. *Society for Neuroscience*, 2011.

[23] W Wang, G P Sudre, Y Xu, R E Kass, J L Collinger, A D Degenhart, A I Bagic, and D J Weber. Decoding and Cortical Source Localization for Intended Movement Direction With MEG. *J Neurophysiol*, 104(5):2451–2461, November 2010.